Journal of Medicinal and Nanomaterials Chemistry

Journal homepage: https://jmnc.samipubco.com/

Short Communication

Influence of atomizing voltage on fluorine doped tin oxide *via* spray pyrolysis technique

Ebube G. Agbim[a], Imosobomeh L. Ikhioya[a,b,*], Azibuike J. Ekpunobi[a]

[a] *Department of Physics And Industrial Physics, Faculty of Physical Science, Nnamdi Azikiwe University, Awka, Nigeria*

[b] *Crystal Growth and Material Science Laboratory/Department of Physics and Astronomy, Faculty of Physical Sciences, University of Nigeria, Nsukka, Nigeria*

ARTICLE INFORMATION

Received: 20 May 2019
Received in revised: 13 July 2019
Accepted: 2 August 2019
Available online: 30 October 2019

DOI: 10.48309/JMNC.2020.1.5

KEYWORDS

Spray Pyrolysis
Fluorine
Tin Oxide
XRD
Optical Properties

ABSTRACT

Synthesis and characterization fluorine-doped tin oxide thin film using spray pyrolysis were coated on a glass substrate by varying the atomizing voltage. The XRD analysis was carried out and the results showed that the deposited films are polycrystalline in nature having the characteristic peaks of tetragonal structure of SnO_2. The observed peaks are (110), (101), (200), (211) and the preferential growth was found to be (110) direction. The I/V plots of the material deposited with 3.8 kV, 4.0 kV and 4.2 kV, which represent sample FT1-FT3 showed a non-linear plot and observed to be a non Ohmic semiconducting material. It was also noticed that as the atomizing voltage of the depositing material increases the thickness of the films increases. The resistivity of the material deposited increases and decreases at 4.0 kV as the atomizing voltage and thickness of the films increases. The electrical conductivity of the material deposited increases with respect to the atomizing voltage and thickness, respectively. It was observed that as the optical absorbance and reflectance decreased the wavelength of the incident radiation and transmittance enhanced as the wavelength of the incident radiation increased and the band gap energy of the films were observed to be at the range of 2.70-3.10 eV.

Corresponding author, email: ikhioyalucky@gmail.com (I.L. Ikhioya).
Tel.: +8038684908.

Graphical Abstract

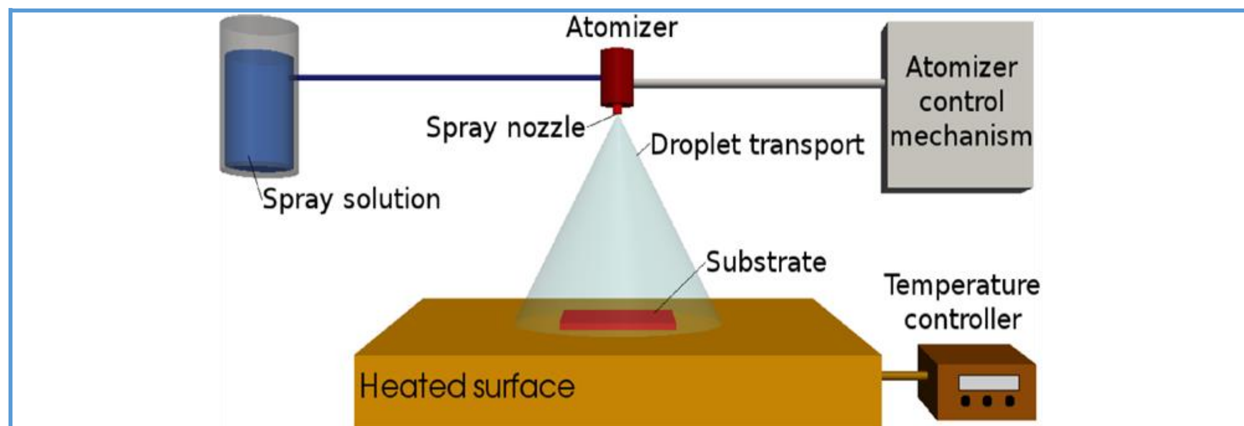

Introduction

Semiconductor thin films has attracted a great deal of attention due to their importance in various fields including, solar cells and gas sensors [1–3]. Transparent conductive oxides of high band gap semiconductors are mechanically hard and can withstand high temperatures. Also wide and direct band gap semiconductor materials are of much interest for blue and ultraviolet (UV) optical devices, such as light-emitting diodes and laser diodes [4–7]. Tin oxide based thin films are good candidate for a number of applications in many fields of research and in various optoelectronic device fabrications [8]. Most important is the thin film application in environmental monitoring through sensing of a number of gases [9]. Tin oxide characteristics for gas sensing applications have been improved through catalytic and impurity doping with a view of improving on its sensitivity to a number of gases as well as its optoelectronic properties [10]. Tin oxide based thin films have been reported to suffer from sensitivity due to the presence of ambient humidity which has been overcome by resistive heating of the thin film gas sensor element [11]. Tin oxide is a wide band gap, non-stoichiometric semiconductor material of n-type conductivity. The conductivity of SnO_2 thin films can be manipulated from normal to degenerate by suitably doping SnO_2 with appropriate amount of halogens [12]. Low electrical resistivity and high visible transmittance are the key elements for solar cell layers, gas sensors, hybrid microelectronics and opto-electronic devices [13]. SnO_2:F coatings can also act as heat mirrors due to their high reflectivity in the infrared range. Among the various transparent conducting oxides, tin oxide (TO) films doped with fluorine or antimony are most promising due to their chemical inertness and mechanical hardness along with low electrical resistivity and good optical transmittance. Tin oxide is the first transparent conductor to have received significant commercialization [14]. The application of thin films in modern technology is widespread. The methods employed for thin-film deposition can be divided into two groups based on the nature of the deposition process viz., physical or chemical. The physical methods include physical vapour deposition (PVD), laser ablation, molecular beam epitaxy, and sputtering. The chemical methods comprise gas-phase deposition methods and solution techniques. The gas-phase methods are chemical vapour deposition (CVD) and atomic layer epitaxy (ALE), while spray pyrolysis, sol-

gel, spin and dip-coating methods employ precursor solutions [14]. Among the various deposition techniques, the spray pyrolysis is well suited for the preparation of doped tin oxide thin films because of its simple and inexpensive experimental arrangement, ease of adding various doping material, reproducibility, high growth rate, and mass production capability [14]. Spray pyrolysis is a processing technique being considered in research to prepare thin and thick films, ceramic coatings, and powders. Unlike many other film deposition techniques, spray pyrolysis represents a very simple and relatively cost-effective processing method (especially with regard to equipment costs). It offers an extremely easy technique for preparing films of any composition. It does not require high-quality substrates or chemicals. The method has been employed for the deposition of dense films, porous films, and for powder production. Even multi layered films can be easily prepared using this versatile technique. Spray pyrolysis has been used for several decades in the glass industry and in solar cell production [14]. Typical spray pyrolysis equipment consists of an atomizer, precursor solution, substrate heater, and temperature controller. The following atomizers are usually used in spray pyrolysis technique: air blast (the liquid is exposed to a stream of air) [15], ultrasonic (ultrasonic frequencies produce the short wavelengths necessary for fine atomization) and electrostatic (the liquid is exposed to a high electric field) [16].

Experimental

Materials and methods

The various materials were used in the fabrication of the films; Glass substrate, Spray pyrolysis machine, Ethanol and water as solvent, Precursor $SnCl_4$ (MERCK), Dopant Ammonium fluoride (BDH), Four-point probe, X-ray diffractometer and UV visible spectrophotometer. Spray pyrolysis technique was used for this deposition. It involves spraying of a solution containing soluble salts of the desired compound onto heated substrates, where the constituents react to form a chemical compound. The chemical reactants used for making solution are selected such that the products other than the desired compound are volatile at the temperature of deposition. Every sprayed droplet reaching the surface of the hot substrate undergoes pyrolytic decomposition and forms a single crystalline or cluster of crystallites as a product. The other volatile by-products and solvents escape in the vapour phase. The substrates provide thermal energy for the thermal decomposition and subsequent recombination of the constituent species.

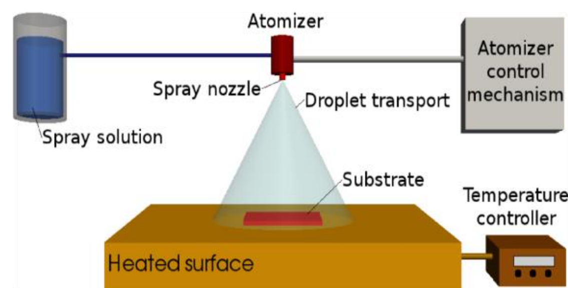

Figure 1. General schematic of a spray pyrolysis deposition process

Substrate (Microscopic glass substrate)

The substrate was a microscopic glass material. The substrates were dipped in acetone, methanol, rinsed with distilled water and later ultra-sonicated for 30 min in acetone solution. Then they were rinsed in distilled water and kept in an oven at 333 K to dry.

Spray process/procedure

The spray process involves optimization of several process parameters. The values of the optimized process parameters are:

Precursor	Flow rate 0.7 mL/min $SnCl_4$ concentration 0.1 mol
Dopant	Ammonium fluoride Concentration (0 to 15 mol %)
Spray- nozzle specification	Outside diameter 0.34 mm Internal diameter 0.18 mm Substrate distance 8 mm
Temperature	400 °C
Atomizing voltage	3.8 kV, 4.0 kV, 4.2 kV
Solvent	Ethanol 90%

Experimental procedure

Thin films of fluorine doped thin oxide were deposited on a transparent glass substrate using $SnCl_4$ dissolved in 90 mL of ethanol and 10 mL of water. The $SnCl_4$ was used as source of Sn while NH_4F as the source of doping impurities. During the deposition, the films were deposited at a constant dopant concentration and voltage rate of 10% and 3.8 KV, respectively. The substrate was attached to the substrate holder, with the temperature regulator; the substrate was heated to the temperature at which that particular sample will be deposited. The voltage was set to 3.8 kV, 4.0 kV and 4.2 kV via the voltage knob and the precursor solution of $SnCl_4$ and NH_4F was passed through the nozzle pump direct to the nozzle. As the mixture gets to the substrate through the nozzle and hits the surface of the substrate, evaporation of the residual solvent takes place, spreading of the droplet and then the salt decomposition $SnO_{2:}$ F was finally deposited on the substrate. Film uniformity was ensured by moving both the nozzle (needle) and the substrate. Different levels of doping were achieved by varying the amount of NH_4F in the precursor solution from 0.1 to 0.3 M. The films with different level of doping were deposited on the glass substrate at 400 °C (Table 1). Uniformity of temperature over the entire substrate and fine sprays were necessary to obtain good quality films which are reproducible. The voltages during spray were 3.8 kV, 4.0 kV, and 4.2 kV with the help of the voltage knob whereas the dopant concentration of NH_4F was kept constant (Table 1). After spraying, the substrates were cooled at room temperature.

Table 1. Variations of voltage parameters for fabrication

Samples	Dopant NH_4F (%)	$SnCl_4$ (mL)	Ethanol (mL)	Voltages (KV)	Temperature (Degree)
FT1	10	20	5	3.8	400
FT2	10	20	5	4.0	400
FT3	10	20	5	4.2	400

Characterization of fabricated films

The fabricated films were characterized using three different instruments for the analysis. The optical analysis were carried out using MT670 UV- visible spectrophotometer where the absorbance of each of the samples was obtain and other optical properties were obtained by calculation. Electrical (I/V) characterization of thin films was done using the four-point probe method at room temperature. The measurements were taken in a square geometry using Keithley 2400 Source Meter. This was carried out at Sheda Science

and Technology Complex, Abuja. The structural characterization of the films was carried out using cu-kal (λ = 1.15418Å) DD-15.5 standard diffractometer, the instrument helped in determining the type of crystal lattice and intensities of diffraction peaks, with the help of data base software supplied by the international center of diffraction data. The characterization was carried out at IThemba LABS Materials Research Department South Africa.

Results and Discussion

Structural analysis

The XRD analysis was carried out to determine the phase angel, crystallite size and dislocation density of the films deposited by varying the deposition temperature of the films., deposition voltage, dopant concentration were kept constant. The XRD patterns of the films prepared by different deposition parameters showed that the deposited films are polycrystalline in nature having the characteristic peak of tetragonal crystal structure. The peaks observed are (110), (101), (200), (211) (Table 2) and among all the peaks the orientation of (110) peak is the highest intensity peak. This is observed in the patterns of all the films with different deposition parameters of SnO_2:F films prepared from $SnCl_4$ precursor, which also revealed the preferential growth along the (110) direction. The crystallite sizes of the deposited SnO_2:F films were determined from Scherer's Equation (1) [17].

$$D = \frac{0.94\lambda}{\beta Cos\theta} \quad (1)$$

where D is the crystallite size in nanometers, β is the full width at half maximum of the diffraction line measured in radians and λ is the wavelength of X-ray used (λ= 1.5418 Å). The dislocation density δ is calculated using Equation 2 [18, 19]. See Figure 2 for the XRD pattern

$$\delta = \frac{1}{D^2} \text{ lines/m}^2 \quad (2)$$

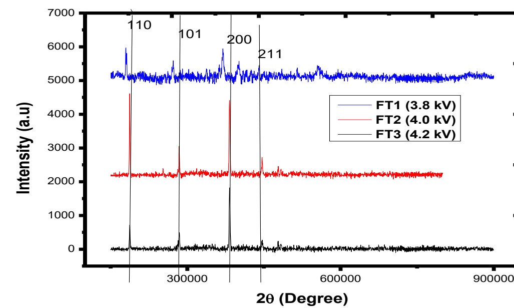

Figure 2. XRD pattern of SnO_2:F

Table 2. Structural parameters of fluorine doped tin oxide

Sample/ Thickness	2θ (degree)	d (spacing) Å	(β) FWHM	(hkl)	Lattice(a) Å	Grain Size(D) nm	Dislocation density(δ)x10^{11} lines/m^2
FT1/ 167.673nm	9.9921	4.943	0.0775	110	4.7309	19.4577	2.6413
	21.7209	4.753	0.0775	101		19.8397	2.5406
	29.6087	4.555	0.0775	200		19.9012	2.5249
	33.4887	4.243	0.0775	211		20.2464	2.4395
FT2/ 169.396nm	9.9921	4.112	0.0775	110		18.9893	2.7732
	21.7209	4.134	0.0775	101		19.3199	2.6791
	29.6087	4.234	0.0775	200		19.4562	2.6417
	33.4887	4.324	0.0775	211		19.5068	2.6280
FT3/ 171.206nm	9.9921	3.294	0.0291	110		50.0067	3.9989
	21.7209	3.285	0.0291	101		50.5956	3.9064
	29.6087	3.265	0.0291	200		51.5843	3.5515
	33.4887	3.243	0.0291	211		52.5620	3.6100

Electrical analysis

The I/V characterization of thin films was done using the four-point probe method at room temperature. The measurements were taken in a square geometry using Keithley 2400 Source Meter. As seen in (Figure 3 and Table 3) the I/V plots of the material deposited at 3.8 kV, 4.0 kV and 4.2 kV, represent sample FT1-FT3 showed a non-linear plot. It was observed to be non Ohmic semiconducting material. It was observed to be non-ohmic semiconducting material. It was also noticed that as the atomizing voltage of the depositing material increased, the thickness of the films was enhanced. The resistivity of the material increased at 4.0 kV as the atomizing voltage and thickness of the films enhanced. The electrical conductivity of the material increased as the atomizing voltage and thickness enhanced [20, 21].

Table 3. Calculated values of resistivity and conductivity

Samples	Thickness, t (nm)	Resistivity, ρ (Ωm)	Conductivity, σ (Ωm)$^{-1}$
FT1 (3.8KV)	167.673	$1.2496 x 10^{4}$	$8.0026 x 10^{-5}$
FT2 (4.0KV)	169.396	$1.1540 x 10^{5}$	$8.6655 x 10^{-6}$
FT3 (4.2KV)	171.206	$2.6891 x 10^{8}$	$3.7187 x 10^{-9}$

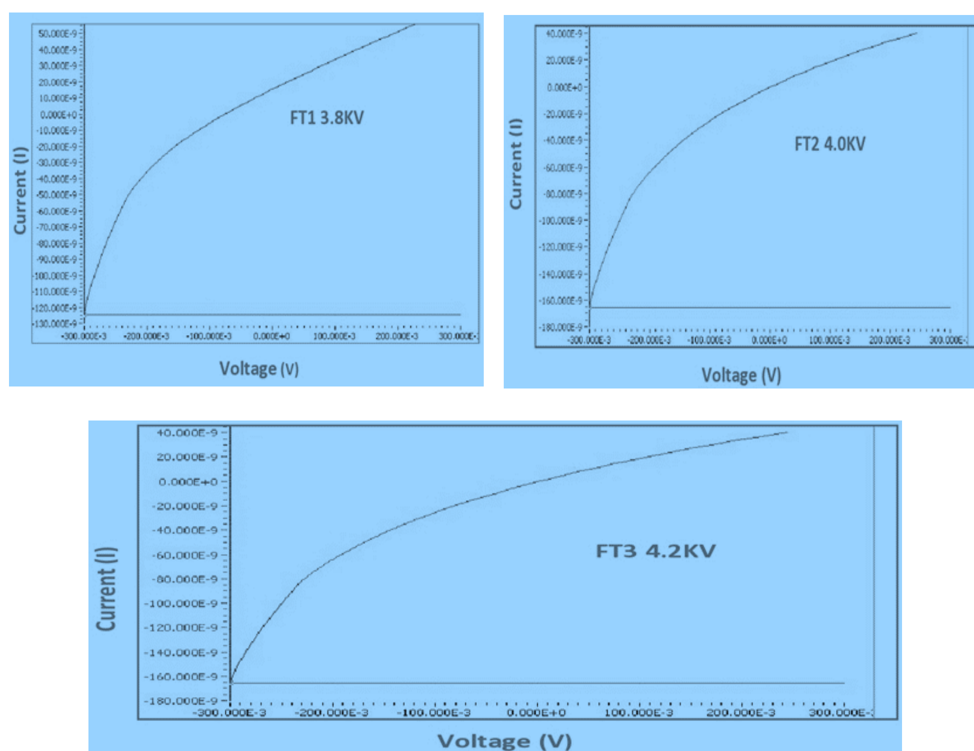

Figure 3. Current versus Voltage plot of sample FT1-FT3

Optical properties

As the optical absorbance decreased the wavelength of the incident radiation raised (Figure 5). It was noticed that, sample FT2 deposited at 4.0 KV emerged the highest absorbance with absorbance value of 0.244 at incident wavelength of 540 nm followed by

sample FT3 deposited at 4.2 KV with absorbance value of 0.233 at incident wavelength of 300 nm. Hence, it is very clear that sample FT1 deposited at 3.8 KV emerged the lowest on the tread with absorbance value of 0.201 at incident wavelength of 340 nm. Therefore, the optical absorbance of the deposited material decreases as the voltage of the deposited material (SnO_4:F) increases with the wavelength of the incident radiation [22–32]. Figure 6 shows that as the optical transmittance increased the wavelength of the incident radiation enhanced. It was noticed that sample FT1 deposited at 3.8 KV emerged the highest transmittance with transmittance value of 0.971 at incident wavelength of 1420 nm followed by sample FT3 deposited at 4.0 KV with transmittance value of 0.951 at incident wavelength of 1480 nm. It was observed that sample FT2 deposited at 4.2 KV recorded the transmittance value of 0.918 at incident wavelength of 1480 nm. Therefore, the optical transmittance of the deposited material decreases as the voltage of the deposited material (SnO_4:F) increases with the wavelength of the incident radiation [33]. From (Figure 7); it was observed that as the optical reflectance decreases the wavelength of the incident radiation increases. It was noticed that sample FT1 deposited at 3.8 KV and sample FT2 deposited at 4.0 KV emerged the highest reflectance with reflectance value of 0.182 at incident wavelength of 540 nm followed by sample FT3 deposited at 4.2 KV with reflectance value of 0.180 at incident wavelength of 380 nm. Hence, the optical reflectance of the deposited material decreases as the voltage of the deposited material (SnO_4:F) increases with the wavelength of the incident radiation [33].

The band gap energy of the deposited material was obtained using

$$\alpha h v = A(h v - E_g)^n$$

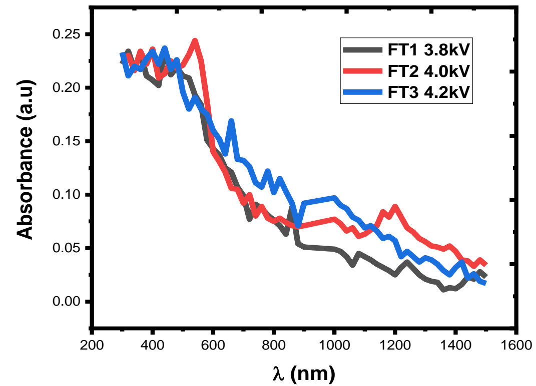

Figure 4. The optical absorbance versus wavelength

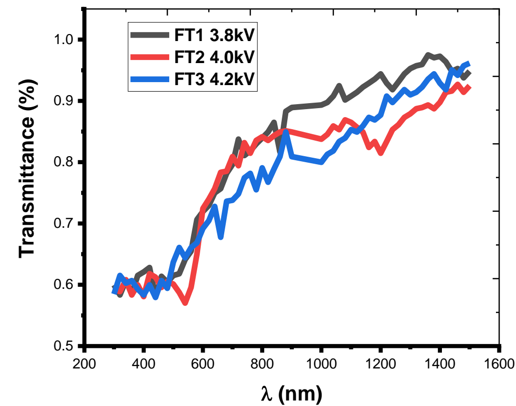

Figure 5. The optical transmittance versus wavelength

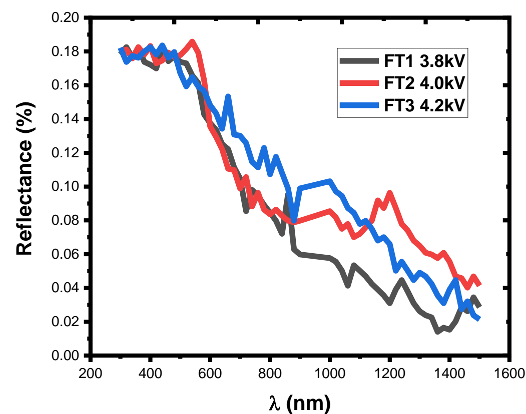

Figure 6. The optical reflectance versus wavelength

Where A is a constant, E_g is the energy band gap of the material deposited (F: SnO_4), h is the

planks constant and $n = \frac{1}{2}$ for direct allowed transition. This relation establishes that a plot of $(\alpha h\nu)^2$ versus $h\nu$ produces a linear pattern the intercept on $h\nu$ axis being the energy band gap, E_g of the thin film. The plot is not direct [22]. The extrapolations of the direct portions of plots to the energy axis give the band gap energy. From (Figure 7) which represents the material deposited at 10conc.-30conc. Recorded energy band gap of 2.70 eV-3.10 eV.

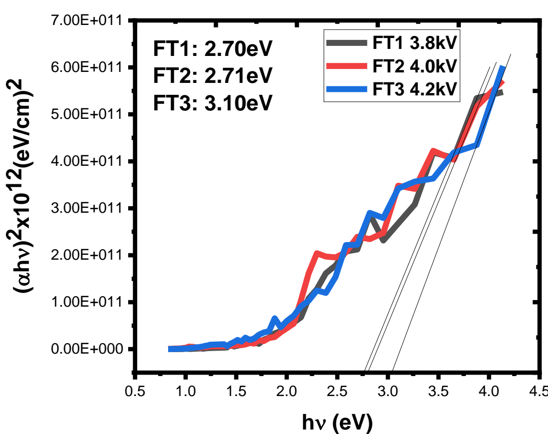

Figure 7. The absorption coefficient square versus photon energy

As seen in Figure 8, the optical refractive index of the deposited material increased and then became steady from refractive index value of 2.5 with increase in photon energy. It was noticed that the sample FT1 deposited at 3.8 KV emerged the highest refractive index with refractive index value of 2.496, sample FT2 deposited at 4.0 KV with refractive index value of 2.496, followed by sample FT3 deposited at 4.2 KV with refractive index value of 2.4895. Hence, the optical refractive index of the deposited material decreases as the voltage of the deposited material (SnO_4:F) increases with photon energy [22–32]. As can be seen in Figure 9, the extinction coefficient increased as the photon energy rose. It was noticed that sample FT1 deposited at 3.8 KV recorded the extinction value of 0.01861 and sample FT2 deposited at 4.0 KV emerged the highest extinction coefficient with extinction coefficient value of 0.0194 followed by sample FT3 deposited at 4.2 KV with extinction coefficient value of 0.01881. Hence, the extinction coefficient of the deposited material increases as the voltage of the deposited material (SnO_4:F) increases with the photon energy. From Figure 10 it was observed that as the optical conductivity increases the photon energy increases. It was noticed that sample FT1 deposited at 3.8 KV, sample FT2 deposited at 4.0 KV and sample FT3 deposited at 4.2 KV follows the trend and recorded optical conductivity value of 4.6154E+13 Hence, the optical conductivity of the deposited material increases as the voltage of the deposited material (SnO_4:F) increases with the photon energy [22–32].

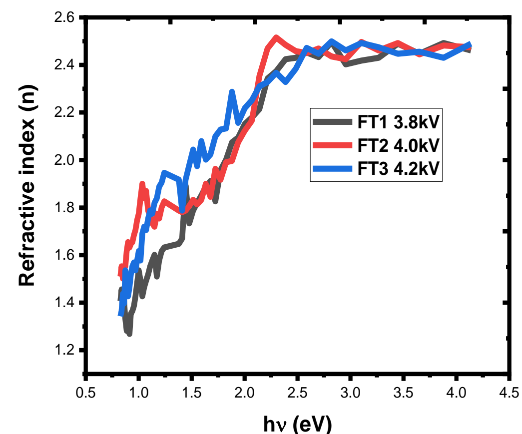

Figure 8. The refractive index versus photon energy

Conclusion

The fluorine doped thin oxide was deposited on a transparent glass substrate using spray pyro lysis technique. The fabricated films were characterized using three different instruments for the analysis. The optical analysis were carri-

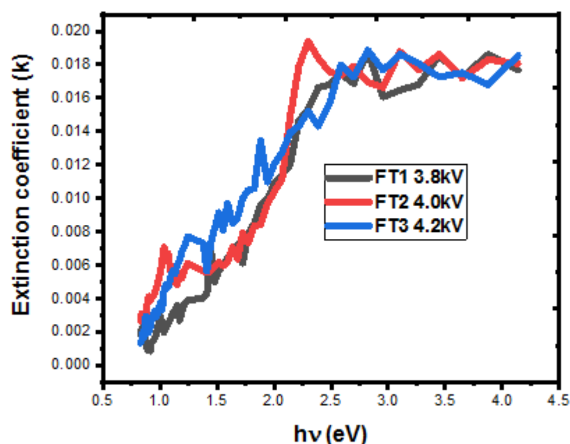

Figure 9. The extinction coefficient versus photon energy

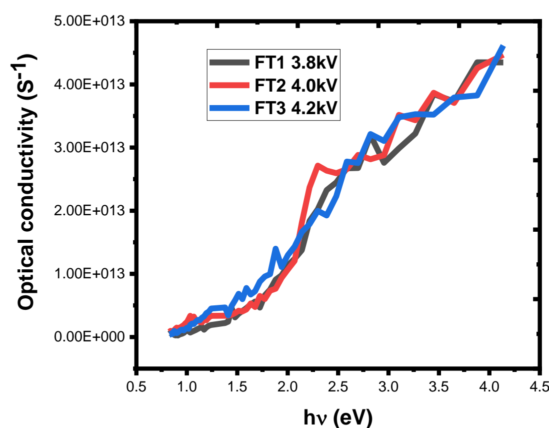

Figure 10. The optical conductivity versus photon energy

ed out using MT670 UV- visible spectrophotometer where the absorbance of each of the samples was obtain and other optical properties were obtained by calculation. Electrical (I/V) characterization of the thin films was performed using the four-point probe method at room temperature, and X-ray diffraction (XRD) analysis was used to evaluate the phases present in the material. The results showed that the deposited films are polycrystalline in nature, having the characteristic peaks of tetragonal structure of SnO_2. The observed peaks are (110), (101), (200), (211) and the preferential growth was found to be (110) direction. The I/V plots of the material deposited with 3.8 kV, 4.0 kV and 4.2 kV, which represent sample FT1-FT3 showed a non-linear plot and observed to be a non Ohmic semiconducting material. It was also noticed that as the atomizing voltage of the depositing material increases the thickness of the films increases. The resistivity of the material deposited increases and decreases at 4.0 kV as the atomizing voltage and thickness of the films increases. The electrical conductivity of the material deposited increases with respect to the atomizing voltage and thickness respectively. It was observed that as the optical absorbance and reflectance decreased the wavelength of the incident radiation and transmittance enhanced as the wavelength of the incident radiation increased and the band gap energy of the films were observed to be at the range of 2.70-3.10 eV.

Acknowledgements

The authors are grateful to the staff of iThemba Laboratory of Materials Research Department South Africa, the staff of energy centre, ABU-Zaria, and finally the Kaduna Polytechnic Centre for Minerals Research and Development Science and Technology Education Post-basic.

Disclosure Statement

No potential conflict of interest was reported by the authors.

References

[1]. Shanthi S., Subramanian C., Ramasamy P. *Journal of Crystal Growth*, 1999, **197**:858

[2]. Abdullahi S., Moreh A.U., Hamza B., Wara M.A., Kamaluddeen H., Kebbe M.A., Monsuorat U.F. *International Journal of Recent Research in Physics and Chemical Sciences*, 2015, **1**:1

[3]. Chamberlin R.R., Skarman J.S. *Journal of the Electrochemical Society*, 1966, **113**:86

[4]. Filipovic L., Siegfried S., Giorgio C.M., Elise B., Stephan S., Anton K., Jordi T., Jochen K., Jorg S., Franz S. *Microelectronics Engineering*, 2013, **117**:57

[5]. Hongli Z. *International Journal of Applied Glass Science,* 2013, **4**:242

[6]. Jariwala C., Dhivya M., Rane1 R., Chauhan N., Rayjada P.A., Raole P.M., John P.I. *Journal of Nano and Electronics Physics*, 2013, **5**:1

[7]. Jaworek A., Sobczyk A.T., Krupa A., Lackowski M., Czech T. *Journal of Technical Sciences,* 2009, **57**:63

[8]. Babar A.R., Shinde S., Moholkar A.V., Bhosale C.H., Kim J.H., Rajpure K.Y. *Journal of Semiconductors*, 2011, **32**:1

[9]. Patrick M.M., Musembi R., Munji M., Odari B., Munguti L., Ntilakigwa A.A., Nguu J., Aduda B., Muthoka B. *Advances in materials,* 2015, **4**:51

[10]. Mwathe P.M., Musembi R., Munji M., Odari B., Munguti L., Ntilakigwa A.A., Nguu J., Aduda B., Muthoka B. *Advances In Materials*, 2014a, **3**:38

[11]. Odari B.M., Musembi R.J., Mageto M.J., Othieno H., Gaitho F., Mghendi M., Muramba V. *American Journal of Materials Science.,* 2013, **3**:91

[12]. Subramanian N.S., Santhi B., Sundareswaran S., Venkatakrishnan K.S. *Metal-Organic and Nano-Metal Chemistry*., 2006, **36**:131

[13]. Ravichandran k., Muruganantham G., Sakthivel B., Philominathan P. *Journal of Ovonic Research*, 2009, **5**:63

[14]. Dainius P., Ludwig J.G. *Journal of Electroceramics,* 2005, **14**:103

[15]. Balkenende A.R., Bogaerts A., Scholtz J.J., Tijburg R.M., Willems H. *Philips Journal of Research*, 1996, **50**:365

[16]. Jaworek A., Sobczyk A.T., Krupa A., Lackowski M., Czech T. *Journal of Technical Sciences,* 2009, **57**:63

[17]. Kandasamy P., Lourdasamy A. *International Journal of Physics*, 2014, **9**:261

[18]. Yadav A.A., Masumdar E.U., Moholkar A.V., Neumann-Spallart M., Rajpure K.Y., Bhosale C.H. *J. Alloys Compd*., 2009, **488**:350

[19]. Noh S.I., Ahn H.J., Riu D.H. *Ceramics Int*., 2012, **38**:3735

[20]. Chantarat N., Yu-Wei C., Shu-Han H., Chin-Ching L., Mei-Ching C., San-Yuan C. *ECS Journal of Solid State Science and Technology*, 2013, **2**:131

[21]. Arle R.N., Khatik B.L. *International Journal of Chemical and Physical Sciences,* 2014, **3**:83

[22]. Agbim E.G., Ikhioya I.L., Agbakwuru C.B., Oparaku O., Ugbaja C.M. *International Journal of Scientific & Engineering Research*, 2019, **10**:707

[23]. Sharma A., Prakah D., Verma K.D. *Optoelectronics and Advanced Materials-Rapid Communications*, 2007, **1**:683

[24]. Jeyasubramanian K.T., Gokul S.R. *Achievers of Material Science and Engineering*, 2016, **78**:66

[25]. Kar S., Kundoo S. *International Journal of Science and Research*, 2015, **4**:530

[26]. Karthick P., Divya V., Suja S., Sridharan M., Jeyadheepan K., *Asian Journal of Applied Sciences*, 2015, **8**:259

[27]. Kandasamy P., Lourdasamy A. *International Journal of Physics*, 2014, **9**:261

[28]. Napi M.L., Maarof M.F., SoonC.F., Nayan N., Fazli I.M., Hamed K.A, Mokhtar S.M., Seng N.K., Ahmad M.K., Suriani A.B., Mohamed A. *Journal of Engineering and Applied Science*, 2016, **11**:8800

[29]. Saipriya M., Sultan R., Singh I. *Physica B*: 2011, **406**:812

[30]. Yadav A.A., MasumdarE.U., Moholkar A.V., Neumann-Spallart M., Rajpure K.Y., Bhosale C.H. *J. Alloys Compd*, 2009, **488**:350

[31]. Ziad Y. B, Kelly P. J., Glen W., Boardman J. *Coatings,* 2014, **4**:732

[32]. Agbim E. G., Ikhioya I.L., Ekpunobi A.J. *IOSR Journal of Applied Physics,* 2019, **11**:70

[33]. Kim K.S., Yoon S.Y., Lee W.J., Kim K.H. *Surface and Coatings Technology*, 2001, **138**:229

How to cite this manuscript: Ebube G. Agbim, Imosobomeh L. Ikhioya*, Azibuike J. Ekpunobi. Influence of atomizing voltage on fluorine doped tin oxide *via* spray pyrolysis technique. *Journal of Medicinal and Nanomaterials Chemistry*, 2(1) 2020, 47-57. DOI: 10.48309/JMNC.2020.1.5